Renewable Energy 252 (2025) 123545

Contents lists available at ScienceDirect

Renewable Energy

journal homepage: www.elsevier.com/locate/renene

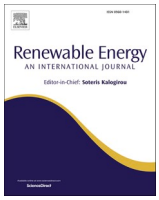

Accelerating geological gas storage simulations: A novel and efficient gases-brine phase equilibrium calculation algorithm

Chaojie Di [a,b], Yizheng Wei [b], Haoming Ma [c], Peng Deng [a], Benjieming Liu [d], Kun Wang [e], Long Peng [f], Zhangxin Chen [d,a,*]

[a] University of Calgary, 2500 University Dr NW, Calgary, AB, Canada
[b] Computer Modelling Group Ltd., 3710 33 St NW, Calgary, AB, Canada
[c] Hildebrand Department of Petroleum and Geosystems Engineering, University of Texas at Austin, Austin, TX, 78712, USA
[d] Ningbo Institute of Digital Twin, Eastern Institute of Technology, 568 Zhuangshi St, Zhenhai District, Ningbo, Zhejiang, PR China
[e] Amazon.com, Inc., 40 King St W 47th Floor, Toronto, ON, Canada
[f] CNPC R&D (DIFC) Company Limited, Dubai, 415147, United Arab Emirates

ARTICLE INFO

Keywords:
Geological gas storage
Gases-brine fluid model
Stability analysis bypassing
Numerical reservoir simulation

ABSTRACT

Geological carbon sequestration (GCS) and gas energy storage in water-bearing formations, one of the most promising methods of Carbon Capture, Utilization, and Storage (CCUS), offers a permanent and reliable solution for mitigating climate change. Although reservoir simulation is widely employed to evaluate GCS projects, its high computational cost, driven by the complexity of phase equilibrium calculations, poses a challenge to obtain timely assessments. To address this, we propose an innovative Adaptive Saturated Composition (ASC) algorithm to bypass unnecessary stability analyses, therefore reducing the computational expenses of gases-brine phase equilibrium calculations in GCS simulation. The ASC algorithm relies on pre-calculated binary gas-brine data and is extended to multicomponent systems (CH_4, N_2, H_2S, CO_2) through a mixing rule. We performed extensive tests under varying underground conditions, demonstrating that the proposed ASC algorithm offers superior efficiency, accuracy and scalability compared to existing algorithms. It eliminates over 99.9 % of unnecessary stability analyses in binary systems and reduces their frequency by over 93 % in multicomponent gas systems. Remarkably, the ASC algorithm achieves accurate detection of phase transitions across all tested scenarios. Moreover, it is widely applicable in most of water-bearing geological gas storage scenarios, including natural gas storage, geological CO_2/air energy storage, and CO_2-based geothermal systems.

1. Introduction

Rising concerns about climate change have elevated geological carbon storage to an urgent global priority for reducing greenhouse gas emissions [1]. Geological CO_2 storage (GCS) involves injecting CO_2 into deep saline aquifers [2], depleted oil reservoirs [3], gas reservoirs [4], geothermal reservoirs [5], and coal seams [6], where it is stored securely over geological timescales. Fig. 1 illustrates the schematic of geological CO_2 sequestration and CO_2 energy storage within a deep saline aquifer. Deep saline aquifers are widely regarded as the most promising storage sites due to their vast capacity and widespread distribution [7]. Numerical simulation of GCS is crucial for understanding long-term storage stability [8] and environmental impact [9]. In GCS simulations, compositional fluid models [10] are widely used to predict the complex interactions between multi-component gas, brine, and underground formations [11]. However, these models are computationally intensive, owing to the considerable computational power required for phase equilibrium calculations [12]. The growing demand for large-scale carbon storage modeling highlights the importance of improving the speed and stability of these calculations to reduce computational resource expenditure. This study focuses on accelerating the phase equilibrium calculations during the GCS simulations. Specifically, we propose a simple, effective, and accurate pre-assessment algorithm to skip unnecessary stability analyses, which is a key component of phase equilibrium calculations (see Fig. 2).

In CO_2 storage simulations, the fluid phase equilibrium algorithm is always time-consuming due to its complexity and frequently repeated calculations [13]. For example, a large-scale carbon storage simulation

* Corresponding author. Ningbo Institute of Digital Twin, Eastern Institute of Technology, 568 Zhuangshi St, Zhenhai District, Ningbo, Zhejiang, PR China.
E-mail address: zhachen@ucalgary.ca (Z. Chen).

https://doi.org/10.1016/j.renene.2025.123545
Received 31 January 2025; Received in revised form 11 May 2025; Accepted 21 May 2025
Available online 24 May 2025

may require millions or even billions of phase equilibrium calculations, primarily including stability analysis and phase splitting [14]. These calculations consume significant computation resources [15], often accounting for 20 %–50 % of the total Central Processing Unit (CPU) time [12]. For equilibrium calculations, a standard workflow performs stability analysis first, followed by phase splitting calculations [16] only if the result of the stability analysis is unstable [17]. When natural primary variables (pressure, temperature, phase saturations, and component mole fractions) are applied in numerical simulations [18], phase split calculations are typically performed once per block or skipped if grids remain in a single-phase state throughout the simulations. However, the stability analysis is performed for every iteration step until all other phases have appeared in this grid. In this condition, stability analysis takes up nearly all the time required for phase equilibrium calculations, as the number of iteration steps can range from thousands to hundreds of thousands [19]. Consequently, minimizing the frequency of stability analysis is key to accelerating phase equilibrium calculations for large-scale CO_2 storage simulations. It improves simulation speed, enabling higher grid resolution and more detailed simulations. On the other hand, a higher simulation speed allows the exploration of additional CO_2 storage scenarios and optimizes storage strategies more effectively within a limited timeframe. These advancements contribute to the comprehensive simulations of storage strategies, which maximize storage capacity while minimizing the risk of leakage.

Previous studies on underground phase equilibrium calculations have contributed significantly to the understanding and modeling of complex phase behaviors among various reservoir fluid systems. Early research focused on developing accurate thermodynamic models for a hydrocarbon fluid to predict its phase behavior at subsurface conditions [20]. Key contributions include the application of the Peng-Robinson (PR) [21] and Soave-Redlich-Kwong (SRK) [22] equations of state (EOSs) in Pressure-Volume-Temperature (PVT) modeling, which are widely used in petroleum reservoir simulations. However, these traditional methods introduce significant errors when predicting gas-brine systems and are unable to accurately capture gas solubility in brine [10]. To address these limitations, new approaches have been developed for gas-brine two-phase systems. A $\gamma - \phi$ approach calculates the fugacity of the gas and liquid phases using EOSs and Henry's law respectively, to improve accuracy [23]. This approach has shown advantages in stability and speed for binary gas-brine systems. Nevertheless, extending this approach to multicomponent systems remains problematic, as the fugacity calculations of each component in the liquid phase are independent of other gas components. Another commonly used method is the $\phi - \phi$ approach, which predicts both gas and aqueous phase fugacity by adapting PR EOS to better represent gas-brine phase behavior. A widely applied model in this approach is the PR EOS modified by Søride and Whitson, generally referred to as the PR-SW EOS [10]. It requires binary interaction parameters (BIP) correlations derived from experimental data to capture the effects of variations in temperature, pressure, and salinity. The component number in this model has no limitations when the correlations of BIP for each gas component have been derived from sufficient experimental data. Other advanced models, including the Cubic-Plus-Association (CPA) [24] and Perturbed-Chain Statistical Associating Fluid Theory (PC-SAFT) [25] equations of state, have been employed to address the limitations of conventional cubic EOS in predicting the phase behavior of

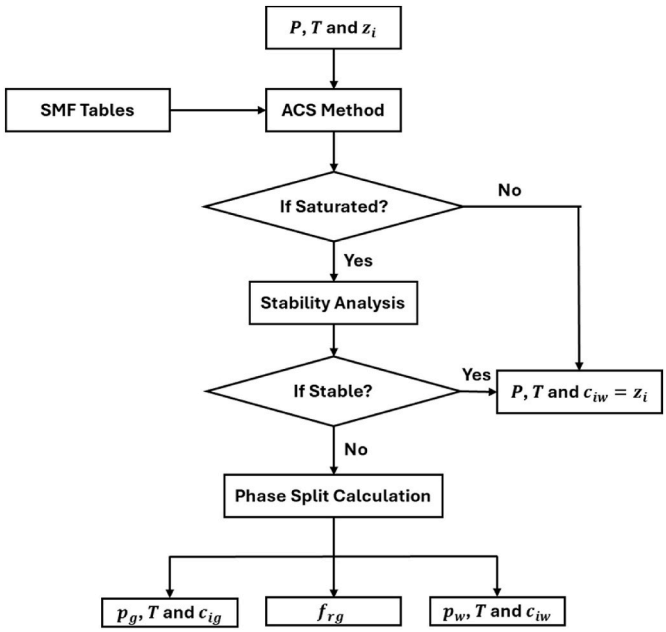

Fig. 2. Phase equilibrium calculation workflow when using the ASC algorithm.

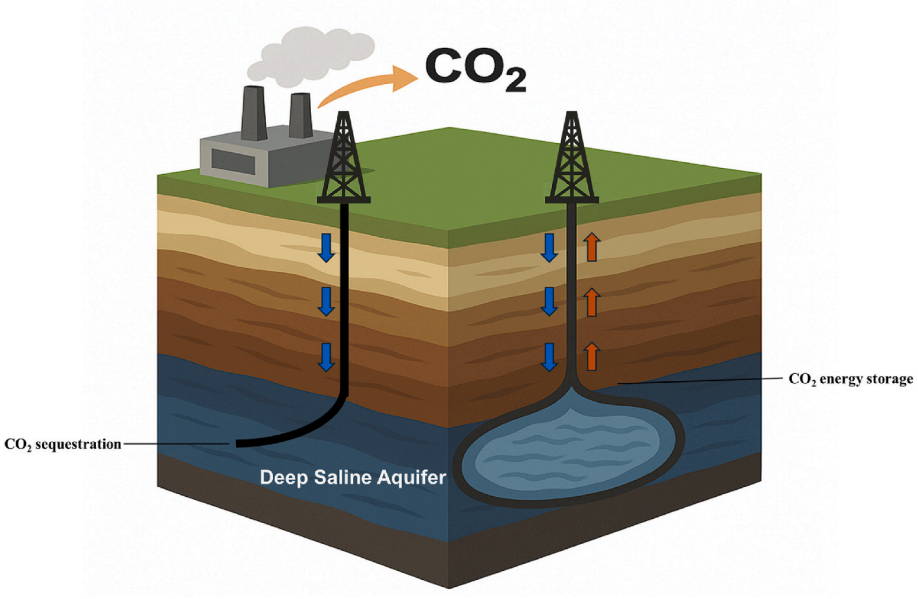

Fig. 1. Geological CO_2 sequestration (GCS) and CO_2 energy storage within deep saline aquifers.

multicomponent gas-brine systems. Although CPA and SAFT models provide improved accuracy in gas-brine fluid modeling, their high computational demands significantly restrict their practical use in large-scale simulations. In contrast, a simpler tabular method simulates the phase equilibrium of gas-brine systems using equilibrium constant or solubility tables [26]. Although this method offers high speed and good stability, it requires recalculating the tables for different gas compositions. Additionally, the accuracy of this approach is often limited, making it less reliable for accurate phase equilibrium predictions.

Numerical reservoir simulation is essential for understanding complex subsurface fluid flow in CO_2 storage [27], enhanced gas recovery [4], and natural gas storage processes [28]. It simulates the interactions between various fluid phases and reservoir rock over a long period under varying pressure, temperature and salinity conditions. Phase equilibrium models are crucial for CO_2 storage simulations, as they determine the composition of gas and aqueous phases, which directly affects predictions of storage capacity [29], injectivity [30], and potential leakage [31]. The complexity of CPA and PC-SAFT results in significantly longer computation time compared to a simpler cubic EOS. Therefore, their application in large-scale reservoir simulations remains limited [32]. In commercial reservoir simulators, $\gamma-\phi$ [26] and $\phi-\phi$ approaches [33] are commonly applied to achieve a balance between accuracy and efficiency in gas-brine phase equilibrium calculations. The tabular method is often employed as a compromise to reduce computational load, although it sacrifices accuracy in phase behavior predictions [34]. All phase equilibrium models except the tabular approach require stability analysis, which can add substantial computational costs. Consequently, stability analysis bypass algorithms are crucial in improving simulation efficiency. The neighborhood bypassing (NB) algorithm reduces computations by only performing the stability analysis for well grid blocks and the single-phase grid blocks adjacent to two-phase grid blocks [12]. While effective in reducing computational load, it carries risks. It arbitrarily overlooks the stability analysis for a large number of single-phase grid blocks, potentially leading to inaccuracies if phase conditions change unexpectedly [35]. Another approach is shadow region bypassing, which excludes grid blocks unlikely to undergo phase changes by defining a shadow region between the two-phase region and the single-phase region in a phase envelope diagram [36]. The original scaling factor used in this algorithm is not suitable for gas-brine fluid systems. Although subsequent modifications have been made to adapt the scaling factor for greenhouse gas storage simulations, its efficiency is very poor when the component number is increased [14]. The compositional space adaptive tabulation (CSAT) approach stores and reuses tie-lines, which are calculated in advance, to avoid redundant computations [37]. This algorithm demonstrates good applicability across different fluid systems as well as thermal and isothermal conditions. Nonetheless, for different simulation cases, tie-line tables for the CSAT method must be recalculated and its bypassing criteria are varied for different fluid systems. These characteristics of the CSAT method will increase setup time and algorithm complexity.

In this study, we propose an adaptive saturated composition (ASC) algorithm to skip unnecessary stability analyses in carbon storage simulations. This novel algorithm is based on the unique characteristics of gas-brine systems and is independent of existing bypassing algorithms. It requires precomputing binary gas-brine data for various gas components, which can then be applied to multicomponent gas-brine systems using an appropriate mixing rule. Additionally, the data tables can be directly reused in other studies if the same EOS parameters are used, demonstrating better portability and practicality than the CSAT method. Through extensive case studies under a wide range of temperature, pressure, and salinity conditions, our new algorithm demonstrates substantial improvements in computational efficiency and accuracy. For binary systems, it bypasses over 99 % of stability analyses, eliminating nearly all redundant computations. When applied to multicomponent systems, this algorithm avoids at least 93 % of stability analyses, maintaining notable computational savings. These results indicate that our algorithm offers better efficiency compared to the previous Shadow-region Bypassing (SB) approach, especially in binary systems. Furthermore, our algorithm demonstrates a remarkable level of accuracy. Across all test simulation cases, the ASC algorithm achieves 100 % correct detection of phase transitions, successfully eliminating the potential impact of stability analysis bypassing algorithms on simulation stability and reliability. Moreover, our algorithm has broad applicability in geological engineering scenarios involving gas-brine systems, including geological natural gas storage, compressed air [38] and CO_2 energy storage [39] in subsurface formation, and CO_2-based geothermal energy exploitation [40]. By improving computational efficiency, it allows scientists and engineers to examine a wider range of carbon storage scenarios, contributing to the optimization of storage strategies.

2. Methodology and theory

This section outlines the methodologies and theoretical foundations applied in this study. It is divided into two subsections. The first subsection describes the mathematical model for geological carbon storage (GCS) and gas-brine fluid modeling, including the mole conservation equations and phase equilibrium calculation algorithms. The second subsection introduces the adaptive saturated composition (ASC) algorithm for stability analyses bypassing, detailing its development and implementation in a GCS simulator.

2.1. Mathematical model of GCS and phase equilibrium calculation

Geological carbon storage (GCS) involves injecting CO_2 into subsurface formations such as deep saline aquifers or depleted reservoirs, where thermodynamic equilibrium plays a critical role in accurately simulating fluid phase behavior. The selection of an appropriate fluid model depends on the storage environment. For CO_2 stored in saline aquifers, a black-oil formulation is often preferred due to its low computational demands. However, when CO_2 contains impurities or is stored in depleted gas reservoirs, the black-oil approach is inadequate as it cannot accurately capture the solubility of different gas components in brine. In these scenarios, compositional models are employed to describe the complex multi-component gas-brine phase behavior. We assume the coexistence of aqueous and gas phases in the underground formation. Gas components can dissolve in the aqueous phase, and water can volatilize into the CO_2-rich phase. The unified molar conservation equation for gas and water components is expressed as [14]:

$$\nabla\cdot\left(c_{iw}\rho_w\boldsymbol{v}_w + c_{ig}\rho_g\boldsymbol{v}_g\right) + \frac{\partial\left(\phi\left[c_{iw}\rho_w S_w + c_{ig}\rho_g S_g\right]\right)}{\partial t} = q_i, i = 1,\ldots,n_g, a \tag{1}$$

where c_i is the mole fraction of i-th component, $\boldsymbol{v}$ denotes the phase volumetric velocity, ρ represents the molar density, ϕ denotes rock porosity, S refers to phase saturation, t is time, q represents molar flux, n_g is the gas component number, a denotes the water component. The subscripts g, w indicate the CO_2-rich and aqueous phases, respectively. $\boldsymbol{v}$ (volumetric velocity) is described using Darcy's law:

$$\boldsymbol{v}_\alpha = -\frac{\boldsymbol{k}k_{r\alpha}}{\mu_\alpha}\nabla(P_\alpha - \rho_\alpha g Z), \alpha = g, w \tag{2}$$

where $\boldsymbol{k}$ refers to the absolute rock permeability, $k_{r\alpha}$ is the phase relative permeability, μ_α denotes phase viscosity, P is the phase pressure, g represents gravity acceleration and Z indicates the grid depth.

Phase equilibrium calculations are a crucial part of GCS simulations, as many parameters in the mass conservation equations—such as phase saturation (S), phase composition (c_i), and fluid properties (density and viscosity)—are directly obtained from these calculations. To accurately model the interactions between CO_2 and brine, we employ the PR-SW EOS method ($\phi-\phi$ approach) in our fluid model. It is based on PR EOS whose PVT relation is given by Ref. [21]:

$$P = \frac{RT}{v - b_m} - \frac{(a\alpha)_m}{v(v + b_m) + b_m(v - b_m)}. \tag{3}$$

b represents dimensional repulsion parameters and v is phase molar volume. The PR-SW EOS introduces a dimensional attraction parameter ($a_i\alpha_i$) for water which is different from PR EOS [10]:

$$(a_i\alpha_i) = \Omega_{ai}\left[1 + 0.453\left[1 - T_{ri}\left(1 - 0.0103c_s^{1.1}\right)\right] + 0.0034\left(T_{ri}^{-3} - 1\right)\right]^2 \frac{(RT_{ci})^2}{P_{ci}}. \tag{4}$$

In Eqns. (3) and (4), c_s indicates the molality of the dissolved salt; T_r is the reduced temperature; R represents the universal gas constant; P_c is the critical pressure; Ω_a refer to the attraction parameter constant. A full formalism of the PR-SW EOS method is detailed in Appendix A. Unlike traditional EOS models, the PR-SW EOS uses different binary interaction parameters (BIPs) for gas and aqueous phases, significantly improving the accuracy of gas solubility predictions. In this study, we focus on the phase equilibrium calculations of CO_2, H_2S, CH_4, N_2 and H_2O mixture using the PR-SW EOS. Other hydrocarbon gases reported in the original literature were excluded from this study because their solubility in brine is very low. The required BIPs for the above gases in the aqueous phase can be calculated using the following equations [10].

$$k^{AQ}_{H_2S,H_2O} = -0.20441 + 0.23426T_r; \tag{5}$$

$$k^{AQ}_{N_2,H_2O} = -1.70235\left(1 + 2.5587 \times 10^{-2}c_s^{0.75}\right) + 0.44338\left(1 + 0.08126c_s^{0.75}\right)T_r; \tag{6}$$

$$k^{AQ}_{CO_2,H_2O} = -0.31092\left(1 + 0.15587c_s^{0.7505}\right) + 0.2358\left(1 + 0.17837c_s^{0.979}\right)T_r - 21.2566\exp(-6.7222T_r - c_s); \tag{7}$$

$$k^{AQ}_{CH_4,H_2O} = \left(1.112 - 1.7369\omega^{-0.1}\right)\left(1 + 4.7863 \times 10^{-13}\omega^4 c_s\right) + (1.1001 + 0.836\omega)\left(1 + 1.438 \times 10^{-2}c_s\right)T_r - (0.15742 + 1.0988\omega)\left(1 + 2.1547 \times 10^{-3}c_s\right)T_r^2. \tag{8}$$

In the non-aqueous phase, the BIPs for CO_2, CH_4 and N_2 are constants which are $k^{NA}_{CO_2,H_2O} = 0.1896$, $k^{NA}_{CH_4,H_2O} = 0.485$ and $k^{NA}_{N_2,H_2O} = 0.4778$, respectively. For H_2S, the BIP is given by Ref. [10]:

$$k^{NA}_{H_2S,H_2O} = 0.19031 + 0.05965T_r. \tag{9}$$

Standard phase equilibrium calculations involve a sequential process of stability analysis and phase split calculations to determine fluid phase behavior under given temperature, pressure, salinity and composition conditions. This process is repeated for each grid block during every iteration step, with phase split calculations only conducted for unstable blocks. The detailed algorithms for stability analysis and phase split calculations used in this study are provided in Appendices B and C, respectively.

2.2. Adaptive saturated composition (ASC) algorithm

Stability analysis is conducted to determine whether a grid block is in a single-phase state. If instability is detected, flash calculations are performed to compute phase transitions and obtain the phase compositions. For two-phase blocks, the disappearance of a phase is determined by checking whether the gas or aqueous phase saturation becomes zero during nonlinear iterations. The ASC algorithm is a novel approach developed in this study to bypass unnecessary stability analyses during carbon storage simulations. It is based on the observation that the saturation mole fractions of gases in binary gas-brine systems provide a reliable criterion for assessing the phase identification of multicomponent gas-brine systems. By comparing the current gas mole fractions (MF) in the grid block with the pre-calculated saturated gas mole fractions (SMF) in the binary systems, the algorithm can accurately identify whether the second phase will appear, allowing skip unnecessary stability analyses. The phase equilibrium simulations are conducted under various temperature, pressure, and salinity conditions using the algorithms discussed in Section 2.1. Through the above calculations, saturated mole fraction tables for binary gas-brine systems are obtained from numerical experiments. These data tables only need to be computed once and can be stored for repeated usage. Appendix D provides a Pseudocode for generating a gas SMF table for gas-brine systems. To calculate the SMF data, we iterate over all temperature, pressure, and salinity points specified in the table. Based on our understanding, the mole fractions of the gases in this research (CO_2, CH_4, H_2S, and N_2) in brine under reservoir conditions do not exceed 0.2 [41]. Therefore, for each phase equilibrium calculation, the mixture composition is initialized as [0.2, 0.8], where the mixture is guaranteed to exist in a two-phase state. As a result, stability analysis is bypassed, and flash calculations are performed directly to determine the saturated gas mole fraction at the given temperature, pressure, and salinity. This approach ensures efficient and accurate generation of the SMF tables.

The SMF tables generated in this study can directly replace phase equilibrium calculations of a binary system. The SMF for a specific grid block under its current temperature, pressure, and salinity conditions can be obtained through interpolation. If the MF exceeds the SMF, the fluid is expected to exist as two phases, and the phase fractions and compositions can then be computed using EOS. This approach is similar to the black-oil model algorithm and the K-value tables method used in the compositional model, neither of which is novel. In this study, we do not intend to use these SMF tables for phase split calculations, as interpolation-based methods inevitably introduce errors. Instead, the SMF tables are solely utilized to determine if stability analysis calculations are necessary. If the MF is larger than the SMF, stability analysis is required; otherwise, it will be skipped. This approach avoids interpolation errors, as the phase compositions are still obtained through a standard phase split calculation. However, when the number of components increases, SMF tables must be recalculated for every component at different fluid compositions, similar to the K-value table and CSAT methods. This would increase the algorithm's complexity and add setup time. To address this, we propose a new approach to extend our ASC algorithm to multicomponent systems without the need for recalculating mixture tables. The binary system SMF tables were used to determine whether the gas components in a mixture are oversaturated. In our algorithm, the system is determined to be single-phase when the following criteria are satisfied:

$$MF_i < SMF_i(P, T, c_s)\frac{z_i}{1 - z_{i,brine}}, i = 1, \ldots, n_g; \tag{10}$$

where z_i is the feed mole fraction for i-th component. If the above criteria are not satisfied, indicating that some components are oversaturated, stability analysis is conducted to accurately assess the phase state. If the system is found to be unstable, phase split calculations are then used to precisely determine the phase fractions and compositions. The following diagram illustrates the phase equilibrium calculation workflow when using the ASC algorithm.

The ASC algorithm offers several key advantages over existing stability analysis bypassing algorithms, making it a practical and effective option for gas-brine phase equilibrium modeling in geological carbon storage (GCS) simulations. These advantages include enhanced scalability, improved accuracy, and significant computational efficiency, as detailed below: 1. The ASC algorithm shows high scalability and setup efficiency for multicomponent gases-brine systems. Unlike the K-value table approach or the CSAT algorithm, which require precomputing extensive tie-line or equilibrium constant tables for specific fluid compositions, the ASC algorithm relies solely on pre-calculated SMF tables for binary systems. These binary SMF tables are computed only once and can be reused across different fluid compositions with a straightforward judgment shown in Eqn. (10). This approach avoids recalculating tables for every new simulation scenario, reducing setup time and simplifying the implementation process. 2. The ASC approach avoids interpolation errors by utilizing a flash calculation procedure when phase transition occurs, ensuring high accuracy even in complex multicomponent systems. 3. The ASC algorithm effectively reduces the computation load of gases-brine phase equilibrium modeling in GCS simulation while maintaining high reliability. This will be further demonstrated in the next Section. Furthermore, the algorithm presented in Section 2.2 has broad applicability in geological engineering scenarios involving gas-brine systems, including geological natural gas storage, compressed air energy storage in subsurface formations, and CO_2-based geothermal energy exploitation. It enables accurate modeling of fluid flow and phase behavior in these subsurface applications, ensuring reliable simulation of complex processes in geological reservoirs.

3. Results and discussions

This Section evaluates the performance of the Adaptive Saturated Composition (ASC) algorithm in geological carbon storage simulations. The results are presented in three sections. First, saturated mole fraction (SMF) obtained from phase equilibrium calculations is analyzed to demonstrate the accuracy and physical consistency of the precomputed SMF tables. Second, based on the computed SMF tables, we discuss the theoretical superiority of the ASC algorithm over the shadow region bypassing (SB) algorithm in modeling gas-brine phase behavior. Finally, the advantages of the ASC algorithm are demonstrated through its application in reservoir simulation cases, showcasing its computational efficiency and reliability compared to the SB algorithm. These findings highlight the capability of the ASC algorithm to enhance both the accuracy and efficiency of phase equilibrium calculations in GCS simulations.

3.1. Saturated mole fraction for gas-brine binary systems

The saturated mole fraction (SMF) tables for binary gas-brine systems were generated using the methodology described in Section 2.1. These tables represent the maximum solubility of gas components in brine under various conditions, including temperature (293.15 K–473.15 K), pressure (5 MPa–65 MPa), and salinity (0–6 mol/kg). The dimension of SMF tables for different gases is 241 × 145 × 7, where 241 points for pressure, 145 points for temperature and 7 points for salinity. The SMF tables form the foundation of the ASC algorithm, providing precomputed reference values for stability analysis bypassing. Fig. 3 illustrates the SMF in pure water (at zero salinity), showing how solubility varies with temperature and pressure. The results highlight the strong dependence of gas solubility on temperature and pressure. The solubilities of CO_2, CH_4 and N_2 increase significantly with pressure, as compression enhances gas-liquid interactions. The effect of temperature on solubility, however, is non-monotonic. At lower pressures, solubility decreases with increasing temperature, which can be attributed to the exothermic nature of the dissolution process. However, at higher pressures, this temperature dependence weakens and even reverses in some cases, leading to relatively high solubility at elevated temperatures and pressures. This complex interplay between pressure and temperature is evident in the upper-right region of the figure, where solubility remains substantial despite high temperatures. For H_2S, at lower temperatures, its solubility shows minimal variation with pressure, only increasing significantly with both temperature and pressure once a certain temperature threshold is reached. The above results confirm the physical consistency of the SMF tables and underscore their importance for the Adaptive Saturated Composition (ASC) algorithm. The precomputed SMF values enable the ASC algorithm to accurately capture the phase transitions in gas-brine systems, providing a reliable foundation for stability analysis bypassing in GCS simulations. Additionally, the observed patterns provide valuable insights for optimizing carbon

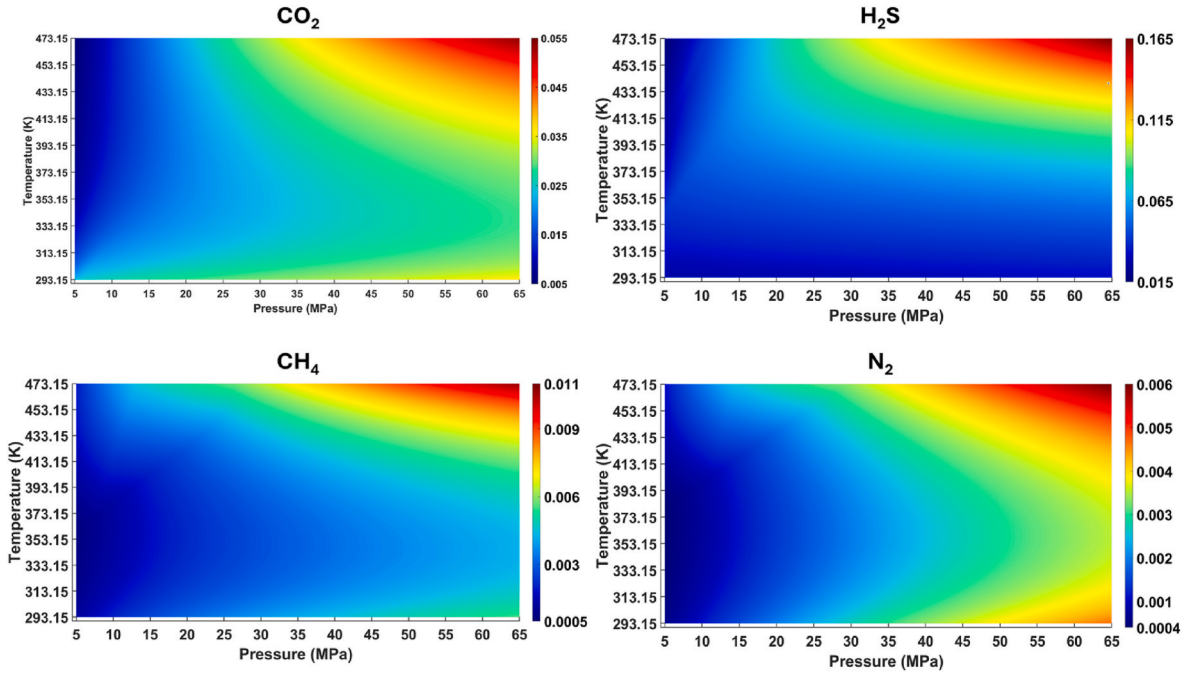

Fig. 3. Saturated gas mole fraction in gas-brine binary systems across a wide range of temperatures and pressures (salinity = 0.0).

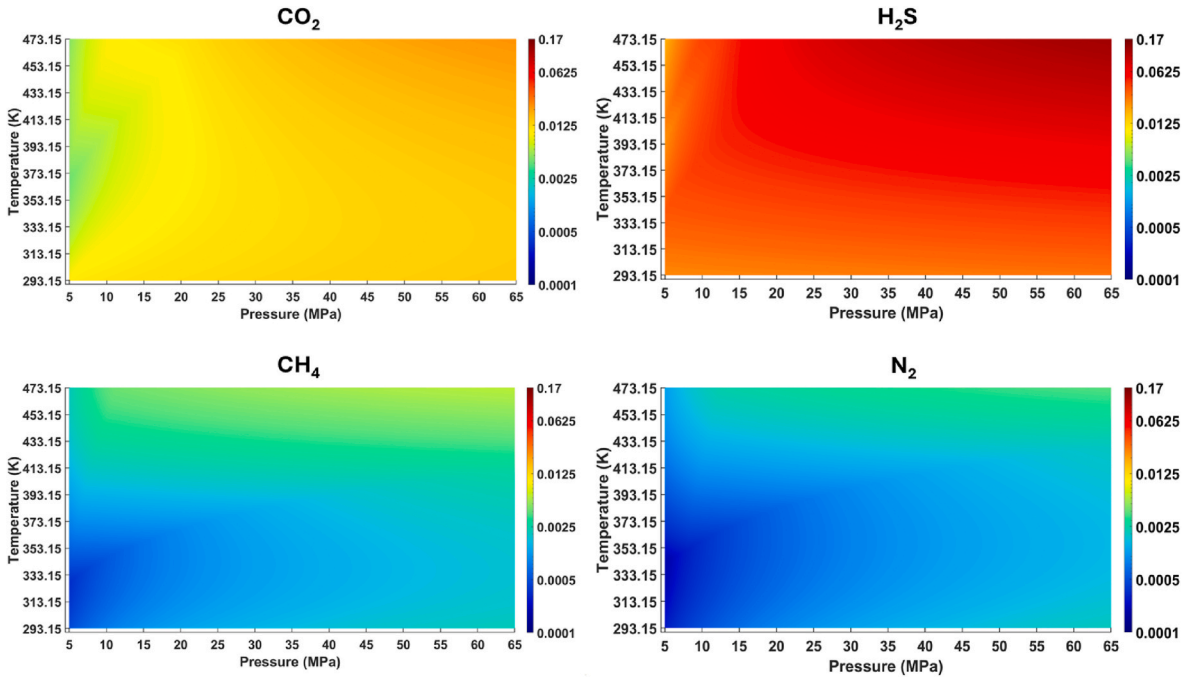

Fig. 4. Saturated gas mole fraction in gas-brine binary systems at salinity = 3.0 with a scale (0.0001–0.17).

storage strategies, suggesting that conditions of high pressure and moderate-to-high temperatures can effectively enhance CO_2 dissolution in brine.

To enable a direct comparison of solubility differences among the four gases, Fig. 4 plots the solubility tables at salinity = 3.0 with a uniform scale (0.0001–0.17). This uniform scaling allows for a direct comparison of the solubility of CO_2, H_2S, CH_4, and N_2 under identical conditions, providing a clearer understanding of their differences. H_2S demonstrates the highest solubility across all conditions, particularly at lower temperatures, where it is significantly more soluble than the other gases. In contrast, CH_4 and N_2 exhibit much lower solubility, with N_2 being the least soluble gas. CO_2 falls between H_2S and the other gases, showing moderate solubility that increases with pressure and temperature. These differences highlight the varying solubility between gas components and brine, emphasizing the importance of accurate phase equilibrium modeling for multi-component systems in carbon storage simulations.

The effect of salinity on the SMF of CO_2 is clearly illustrated in Fig. 5. As salinity increases, a notable decrease in the SMF can be observed across the entire temperature and pressure range. This behavior is primarily attributed to the salting-out effect, where the presence of dissolved salts reduces the solubility of CO_2 in brine by decreasing the free volume of the aqueous phase and competing for molecular interactions. At lower salinity levels, the SMF of CO_2 remains relatively high, with values exceeding 0.05 in high pressure and temperature regions ($P > 50$ MPa and $T > 433$ K). However, as salinity increases, the SMF decreases significantly. The reduction trend is consistent across the temperature-pressure domain, with an average relative reduction in SMF of approximately 80 % in high-salinity cases compared to pure water. For instance, at 55 MPa and 453 K, the SMF decreases from 0.0426 at 0 mol/kg salinity to 0.0081 at 6 mol/kg salinity. This quantified reduction highlights the strong salting-out effect, where higher ionic

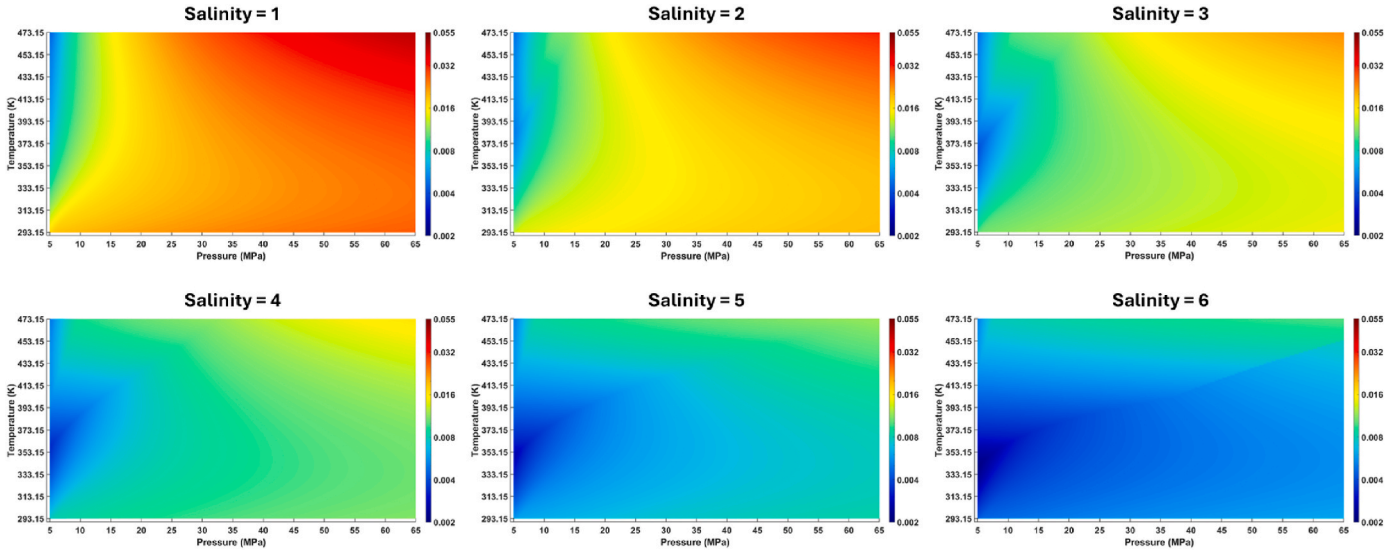

Fig. 5. Saturated gas mole fraction in CO_2-brine binary systems at different salinity (1.0–6.0).

concentrations suppress CO_2 solubility in brine. These findings emphasize the critical role of salinity in accurately predicting phase behavior in geological carbon storage scenarios.

3.2. Theoretical insights of ASC and SB algorithm

In this section, we will utilize SMF tables to reveal the limitations of the existing shadow region bypassing (SB) algorithm in gases-brine phase equilibrium calculations. During carbon storage simulations, the initial fluid composition is typically pure brine, and the smallest eigenvalue (b) in the SB algorithm is usually determined under this composition. Numerical experiments reveal that, regardless of temperature, pressure and salinity, the value of b under pure brine conditions consistently equals 1. Consequently, for carbon storage in brine, the mole fraction for the bypassing criterion of the SB algorithm is simplified to:

$$z_i \geq \frac{1}{\eta} \tag{11}$$

where η is the scaling factor which is typically determined empirically and z_i refers to feed mole fraction. If Eqn. (11) is satisfied, a stability analysis will be performed to determine whether the fluid is in two-phase zones; otherwise, the fluid is directly assumed to be in single-phase zones. To ensure the efficiency of the bypassing algorithm, the scaling factor should be as small as possible. To avoid misclassifying two-phase grid blocks as single-phase grid, $1/\eta$ should not exceed the saturated mole fraction (SMF). The optimal scaling factor (η_{opt}) can thus be obtained from $SMF = 1/\eta_{opt}$, leading to:

$$\eta_{opt} = \frac{1}{SMF(P, T, c_s)} \tag{12}$$

The application of the SB algorithm in gas-brine phase equilibrium calculations is limited. It employs a constant scaling factor (η_{con}) and does not consider the effect of pressure, temperature and salinity. For different gases, the scaling factors are: $\eta_{CO_2} = 100$, $\eta_{H_2S} = 50$, $\eta_{CH_4} = 1000$ and $\eta_{N_2} = 1500$ [14]. These constant values often fail to reflect the actual behavior of gases in the brine, resulting in poor efficiency or bad bypassing. Fig. 6 illustrates the ratio of the optimal scaling factor (OSF) to the constant scaling factor (CSF) for CO_2 under varying temperature, pressure, and salinity conditions. A ratio greater than one indicates that the CSF is too small, which may lead to wrong bypassing in phase equilibrium modeling. Conversely, a ratio of less than one suggests that the CSF is too large, which reduces the efficiency of the bypass algorithm. Maintaining this ratio within the range of 0.8–1.2 strikes a balance between algorithm accuracy and efficiency, ensuring optimal performance for stability analysis bypassing in phase equilibrium calculations. For the CSF to be considered optimal, the OSF/CSF ratio should predominantly lie within the transition region (around 0.8–1.2) in Fig. 6. At lower salinities (1–2 mol/kg), the ratio is primarily in the blue region, indicating that the CSF is overly conservative and leads to reduced efficiency. As salinity increases (3–4 mol/kg), the ratio gradually shifts, with more areas falling into the transition region. However, at low pressures and moderate temperatures, the ratio often exceeds 1.2, suggesting that the CSF becomes too small and leads to more wrong bypassing. As salinity increases to 5–6 mol/kg, the red regions dominate the plot, indicating that the CSF is too small and cannot meet the accuracy requirements. These patterns demonstrate that the CSF is suboptimal for varied formation conditions and further illustrate the demands for a more adaptive approach like the ASC algorithm to achieve better performance across different salinity levels.

Fig. 7 illustrates the OSF/CSF ratio for four gas species at salinity = 3 mol/kg, aiming to evaluate the adaptability and accuracy of the SB algorithm across different gases and conditions. The OSF/CSF ratio map shows that CO_2 has the largest suitable region, where the ratio falls within the ideal range (0.8–1.2), compared to the other gases. CH_4 and N_2 exhibit similar distribution patterns and region sizes. For CO_2, CH_4 and N_2, the suitable regions are limited, with most areas dominated by either blue or red zones. In contrast, H_2S is almost entirely in the blue zone, indicating that the SB algorithm is highly inefficient for H_2S, with significant potential for further optimization. Overall, this comparative analysis reveals that the performance of the SB algorithm heavily depends on the gas species, as the fixed CSF values fail to adapt to the varying phase behavior of different gases.

The analysis of the OSF/CSF ratio for gas-brine binary systems highlights the limitations of using a constant scaling factor in the SB algorithm for gas-brine systems. The ideal regions where the ratio falls within the acceptable range are relatively small, with most areas either undersized (red) or oversized (blue), leading to accuracy compromises or inefficiency. The situation is even more pronounced for H_2S, where the predominantly blue regions indicate that the CSF fails to achieve the necessary efficiency. Furthermore, for multi-component systems, η is determined by the largest CSF among the gas components, which undoubtedly reduces the efficiency of the algorithm [14]. These results underscore the inadequacy of CSF in adapting to varying temperature, pressure, and fluid composition conditions, emphasizing the need for

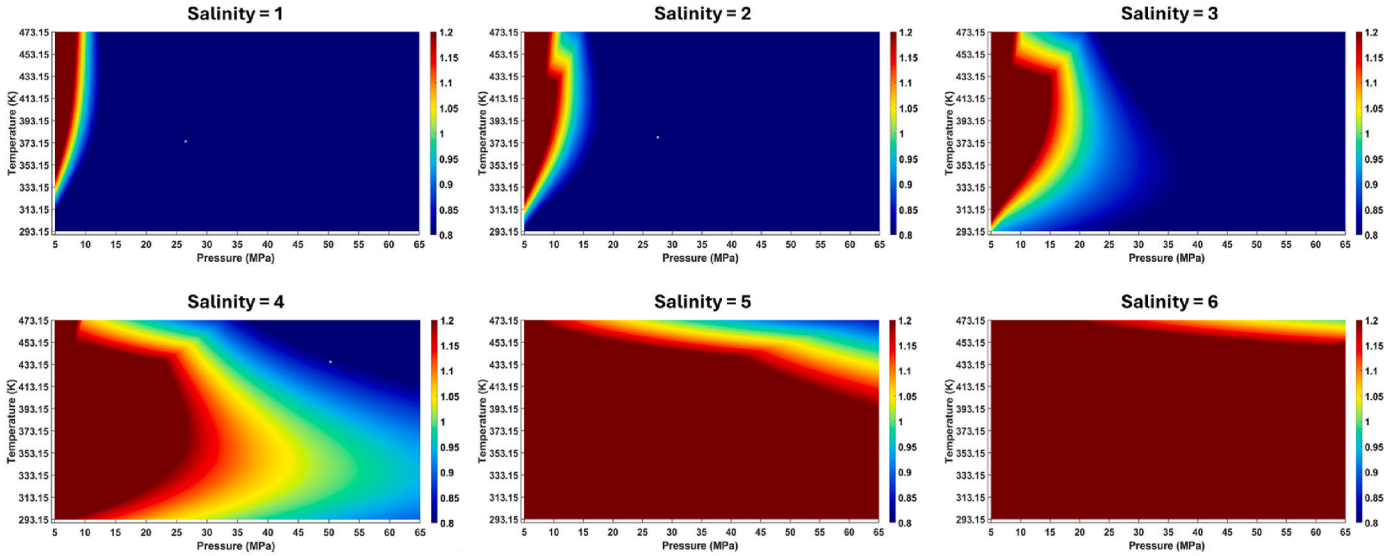

Fig. 6. OSF/CSF ratio for a CO_2-brine system under varying temperature, pressure and salinity.

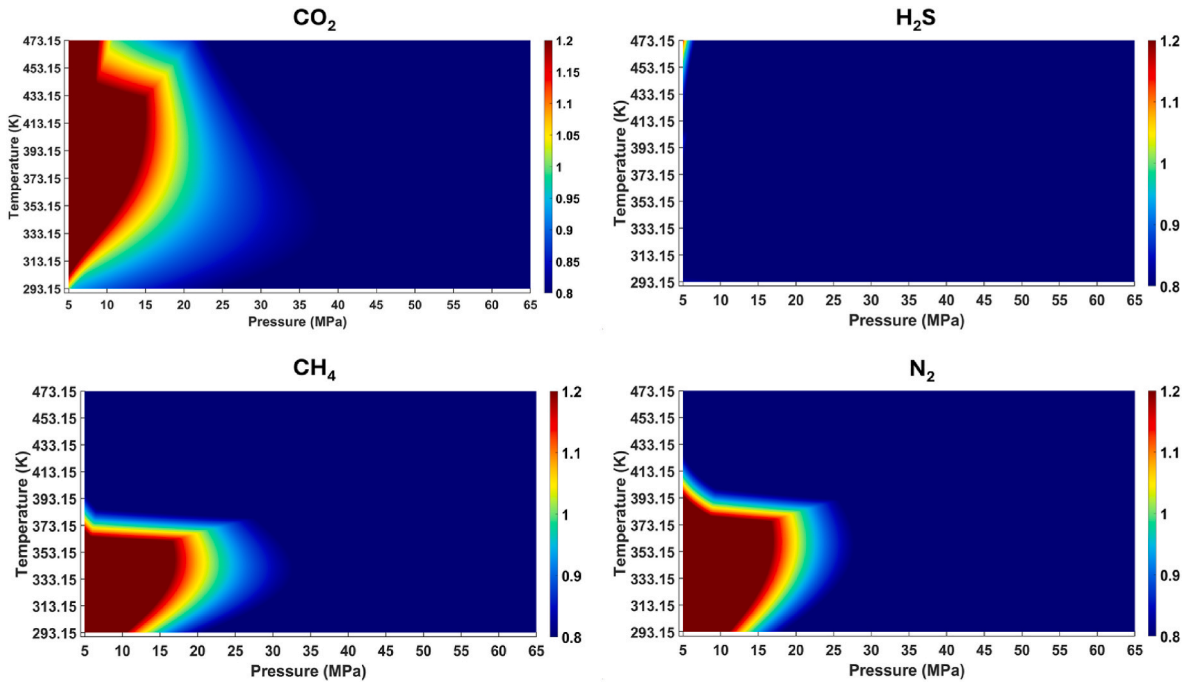

Fig. 7. OSF/CSF ratio for gas-brine systems at salinity = 3.0.

more flexible and adaptive approaches. The ASC algorithm employs the criterion outlined in Eqn. (10) for multicomponent gas-brine systems. This approach ensures that the ASC algorithm maintains high efficiency even when applied to complex fluid compositions, significantly enhancing its applicability and performance in real-world scenarios.

3.3. Application of bypassing algorithm in GCS

This section evaluates the efficiency and accuracy of stability analysis bypassing algorithms in geological carbon storage (GCS) simulations using two key indices: residual stability analysis ratio (RSAR) and bad bypassing number (BBN). RSAR represents the ratio of stability analysis number (SAN) after using a bypassing algorithm to the total number required without bypassing, where lower values indicate greater efficiency. BBN is the number of incorrectly bypassing in cases where phase transitions occur, reflecting the algorithm's accuracy. The SMF tables in Section 2 are used in the following GCS simulation cases. Two GCS simulation models were analyzed: GMGHG005M and SPE11C. GMGHG005M is a homogeneous model with simpler geological conditions and injection operations. It was selected to test the performance improvement of our algorithm under idealized laboratory conditions for a mechanistic study. SPE11C is a more complex model that better represents realistic subsurface conditions, allowing us to confirm the practical value of our algorithm in real-world engineering applications. These evaluations highlight the advantages of the ASC algorithm in enhancing computational efficiency while maintaining reliability in GCS simulations.

3.3.1. GMGHG005M cases

The GMGHG005M case is a benchmark model derived from the CMG-GEM template cases, specifically designed for geological CO_2 storage in a deep saline aquifer. The model is a Cartesian grid system

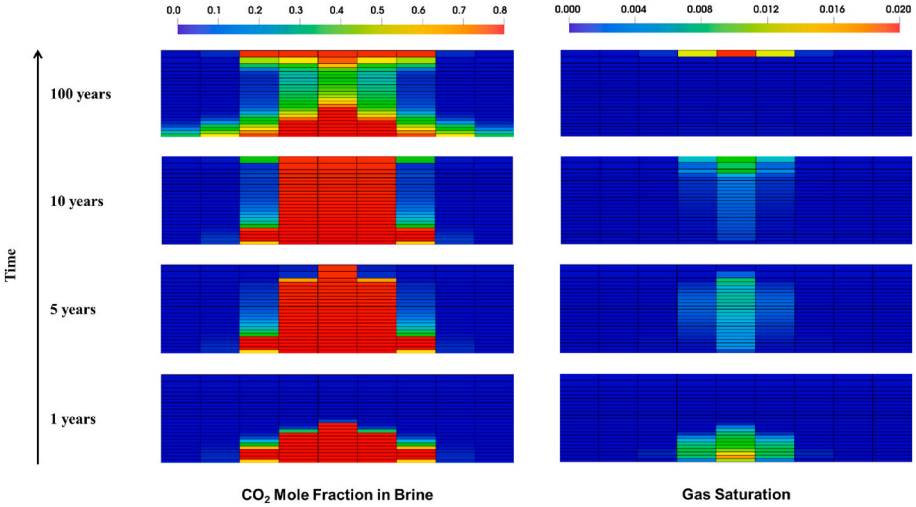

Fig. 8. Distribution of CO_2 in gas and aqueous phases for the first 100 years in a plane of GMGHG005M (at $x = 5$). Note: The results are modified based on our previous work [14].

with dimensions of 9 × 9 × 24, where 9 grid cells are in the x and y directions and 24 grid cells are in the z direction. An injection well is located at the center bottom (x = 5, y = 5, z = 24) of a homogeneous aquifer formation. CO_2 will be injected in the first 25 years, followed by a long-term simulation over 250 years to evaluate CO_2 migration in the underground formation. Further details about the model setup can be found in the CMG template case library [26] or literature [14]. Fig. 8 presents a cross-sectional view of the GMGHG005M model at $x = 5$, showing the spatial distribution of gas saturation (right) and CO_2 mole fraction in brine (left) for the first 100 years. The results illustrate the upward migration of CO_2 due to buoyancy, creating a CO_2 plume that spreads vertically and horizontally. The gas phase accumulates near the top of the formation, while the dissolved CO_2 in brine disperses in a broader area beneath the gas cap. The CO_2 plume occupies a significant portion of the grid cells in this model, leading to a higher frequency of required stability analyses. This requires a high-accuracy bypassing algorithm to ensure that simulation reliability is not compromised. The large sweep area of the CO_2 plume underscores the challenges in balancing the efficiency and accuracy of stability analysis bypassing algorithm in GCS simulations.

We conducted extensive simulations to evaluate the efficiency and accuracy of the ASC algorithm using the GMGHG005M case. Four different injection gases were selected to analyze the impact of gas composition on the algorithm's performance: 100 % CO_2, 95 % CO_2 + 5 % H_2S, 90 % CO_2 + 5 % H_2S + 5 % CH_4, and 85 % CO_2 + 5 % H_2S + 5 % CH_4 + 5 % N_2. For convenience, these fluid systems are referred to as 2C, 3C, 4C, and 5C, based on their component number (gas + water) in the rest part of this paper. To study the effects of temperature and pressure, the aquifer depth was varied across three scenarios: 1000 m, 2000 m, and 3000 m, corresponding to initial temperature and pressure conditions of (318 K, 10 MPa), (348 K, 20 MPa), and (378 K, 30 MPa), respectively. Additionally, salinity levels were tested at 0.00, 2.75, and 5.50 mol/kg. By combining these varied settings, a total of 4 × 3 × 3 = 36 scenarios were evaluated, providing a comprehensive analysis of the ASC algorithm's performance under a wide range of geological and operational conditions.

Fig. 9 shows the RSAR values after applying stability analysis bypassing algorithms. The panels on the left illustrate RSAR under three different temperature conditions (318 K, 348 K, and 378 K), while the panels on the right depict RSAR under three salinity levels (0.00, 2.75, and 5.50 mol/kg). Each panel further categorizes RSAR by component numbers (2C, 3C, 4C, and 5C), allowing an in-depth evaluation of how these parameters influence the efficiency of stability analysis bypassing algorithms. This figure includes RSAR for both the Adaptive Saturated Composition (ASC) algorithm and the shadow region bypassing (SB) algorithm, enabling a direct comparison of their performances for GMGHG005M cases. From the left-side panels, it is evident that RSAR for the SB algorithm decreases with rising temperature, while the ASC algorithm remains relatively stable across different temperatures. The right-side panels reveal that increasing salinity slightly reduces RSAR for

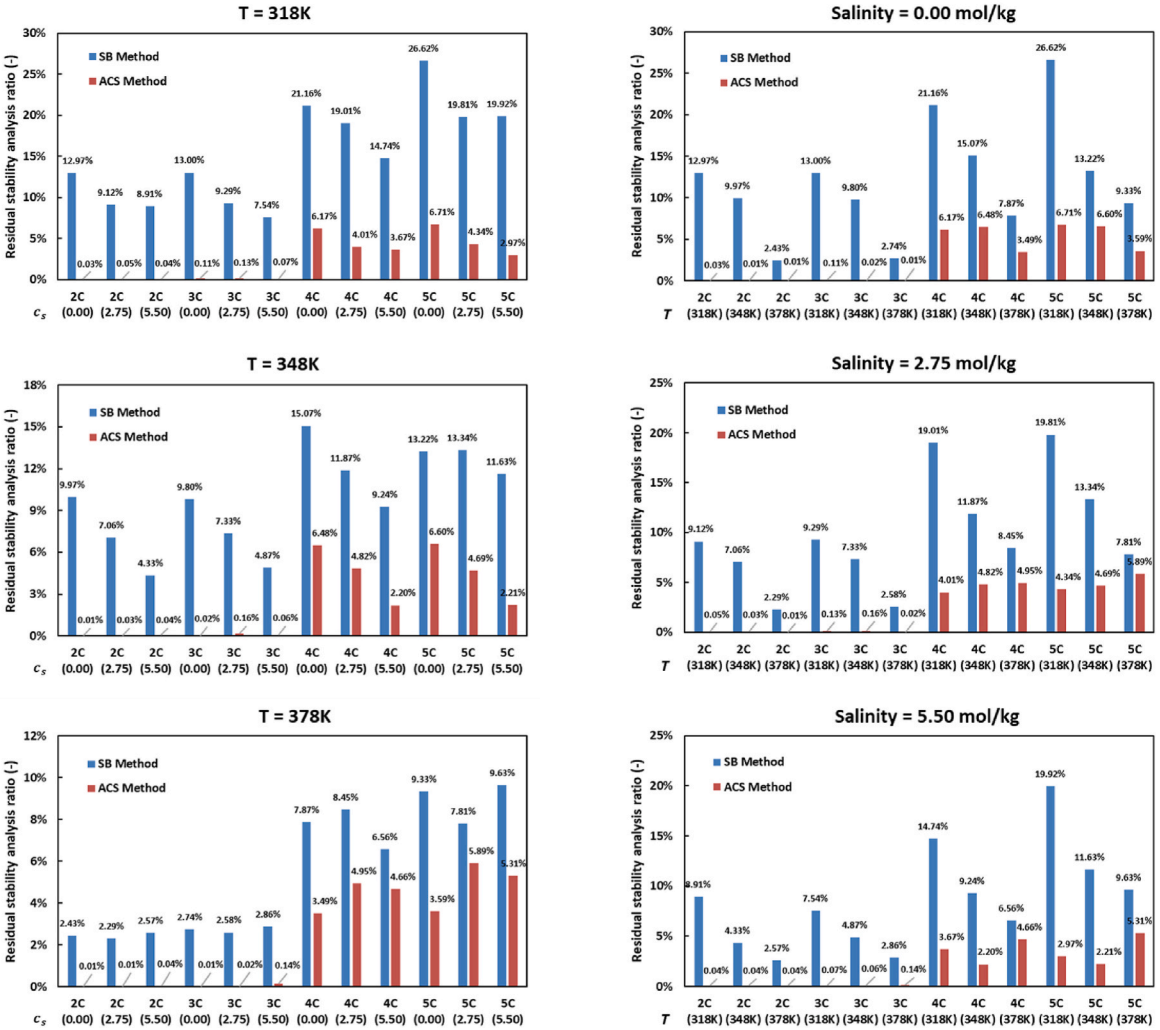

Fig. 9. Residual stability analysis ratio (RSAR) of GMGHG005M cases after using ASC or SB algorithms.

both algorithms, but its impact is quite limited. For the influence of component number, it is notable that the ASC algorithm performs exceptionally well in cases with fewer components (e.g., 2C and 3C), where it almost skips all unnecessary stability analyses. This highlights the superior efficiency of the ASC algorithm in simpler gas compositions compared to the SB algorithm. As the component number increases from 3C to 5C, reflecting the growing complexity of phase equilibrium calculations in multicomponent systems, RSAR increases for both algorithms. However, the ASC algorithm demonstrates better scalability, with RSAR values consistently lower than those of the SB algorithm, regardless of component number. This suggests that the ASC algorithm is more effective at handling complex fluid systems. The results presented in Fig. 9 emphasize the significant computation savings achieved by stability analysis bypassing algorithms in phase equilibrium calculations. While both algorithms reduce the frequency of stability analyses, the ASC algorithm outperforms the SB algorithm in terms of efficiency across all tested conditions.

The accuracy of bypassing algorithms is evaluated for the GMGHG005 cases by analyzing the BBN. The ASC algorithm demonstrates remarkable accuracy, with no bad bypassing observed in any of the tested scenarios. In contrast, the SB algorithm shows varying degrees of bad bypassing across different cases. Table 1 provides a detailed breakdown of bad bypassing numbers (BBN) for the SB algorithm under different reservoir and operational conditions. The table reveals that bad bypassing is more likely to occur in scenarios with fewer component numbers, moderate temperatures, and higher salinity levels. The results highlight the superior accuracy of the ASC algorithm, avoiding bad bypassing and ensuring the reliability of simulation results. This advantage makes the ASC algorithm highly reliable for geological carbon storage simulations, addressing a critical limitation of traditional stability analysis bypassing algorithms.

To further demonstrate the computational advantages of the ASC method, we present a comparative analysis of simulation time using the SB method and the proposed ASC method at a temperature of 318 K, as shown in Fig. 10. The vertical axis represents the residual simulation time as a percentage of the baseline full-stability-analysis simulation across different component numbers (2C–5C) and salinities (0.00, 2.75 and 5.50 wt%). Overall, the ASC method significantly reduces the simulation time across all cases. The time saved by the ASC method typically falls in the range of 20 %–50 %, which is better than that of the SB method. It should be noted, however, that the extent of time reduction may vary across different reservoir simulators, as the proportions of phase equilibrium calculations and the numerical implementation details can differ from one simulator to another. The superior performance of the ASC method can be attributed to two main factors: skipping more unnecessary stability analysis calculations and fewer misjudgments. The SB method tends to provide a wrong phase number in some cases, as described in Table 1, which leads to numerical instability. This, in turn, causes smaller time steps and an increase in the total number of simulation steps (N), directly increasing simulation time. This phenomenon is clearly observed in the 2C-(5.50) and 5C-(0.00) scenarios, where the SB method resulted in 33 and 6 additional time steps, respectively. In these cases, the SB method even increased the overall simulation time compared to the full-stability-analysis baseline, leading to efficiency losses. In contrast, the ASC method maintained its high accuracy and did not suffer from such issues, demonstrating better performance across all test scenarios. These results further validate the ASC method's advantages in accelerating GCS simulations.

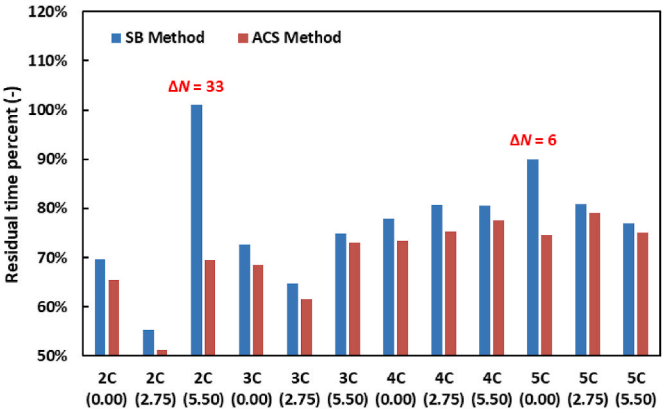

Fig. 10. Residual time percent across different compositions and salinity conditions at $T = 318$ K.

3.3.2. SPE11C case

The SPE11C case is one of the well-known SPE comparative solution projects, which provides benchmark models for evaluating reservoir simulation methods. This case has been widely adapted and modified in studies focusing on CO_2 geological storage due to its realistic representation of the heterogeneity of subsurface formation and long-term simulation requirements. In this study, it uses a corner-point grid system with dimensions of $168 \times 120 \times 20 = 403200$, designed to simulate CO_2 injection into a deep saline aquifer. Two injection wells are positioned at the center of two high-permeability layers within the reservoir. CO_2 was injected at a constant rate for 50 years and 25 years respectively, followed by a post-injection simulation for 1000 years. The geological setup includes heterogeneous permeability and porosity fields, representing realistic subsurface conditions. This is an ideal model for testing the robustness of stability analysis bypassing algorithms in handling heterogeneous and long-term storage simulations. Fig. 11 is a sketch of the benchmark geometry for SPE11C in the reference configuration and its detailed setup information can be found in the literature [42].

Fig. 12 provides a cross-sectional view of the SPE11C model at $y = 10$, illustrating the spatial distribution of gas saturation (right) and CO_2 mole fraction in brine (left) over the simulation period. The simulation captures the injection process from two wells: the first well operates continuously for 50 years, while the second well begins injection at the 25th year and operates until the 50th year. The results reveal distinct migration patterns for CO_2, primarily influenced by buoyancy and the heterogeneous permeability of the reservoir. The CO_2 plume expands vertically and laterally from the injection points, with gas saturation accumulating at the top of the high-permeability layers. Meanwhile, dissolved CO_2 exhibits a broader distribution within the brine phase, spreading over a broader area beneath the gas phase. Compared to the GMGHG005M model, the SPE11C case shows a much lower proportion of grid cells swept by the CO_2 plume. This aligns more closely with

Table 1
Bad bypassing number (BBN) of GMGHG005M cases after using the SB algorithm.

		2 Components			3 Components			4 Components			5 Components		
		Salinity (mol/kg)			Salinity (mol/kg)			Salinity (mol/kg)			Salinity (mol/kg)		
		0	2.75	5.5	0	2.75	5.5	0	2.75	5.5	0	2.75	5.5
T (K)	318	0	0	1197	0	2	719	0	0	48	5	8	12
	348	0	2152	6358	0	360	5583	0	72	107	20	472	84
	378	0	670	2741	0	675	1693	0	52	100	20	52	228

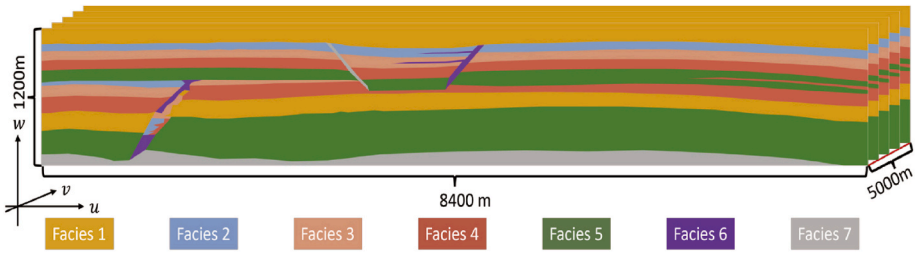

Fig. 11. Sketch of the benchmark geometry for SPE11C in the reference configuration [42].

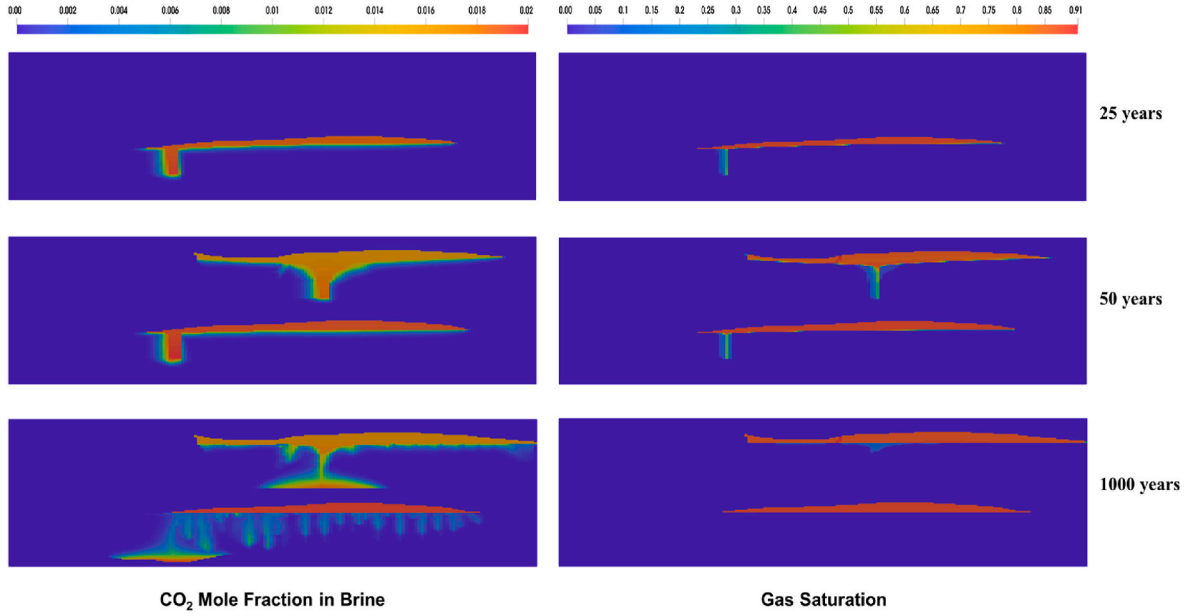

Fig. 12. Distribution of CO_2 in gas and aqueous phases in a plane of the SPE11C model (at $y = 10$).

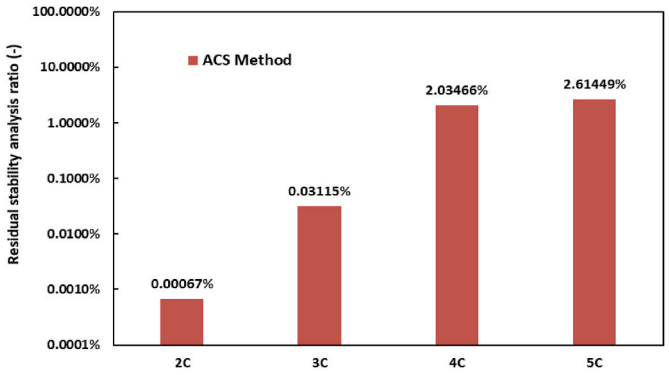

Fig. 13. Residual Stability Analysis Ratio (RSAR) of ASC algorithm for the SPE11C model.

realistic geological storage scenarios, where CO_2 injection impacts are generally localized to specific regions. The lower fraction of affected grid cells suggests fewer stability analyses are necessary, making this case particularly useful for assessing the efficiency of ASC bypassing algorithms.

Fig. 13 illustrates the RSAR values for the SPE11C model under four different injection gas compositions: 100 % CO_2 (2C), 95 % CO_2 + 5 % H_2S (3C), 90 % CO_2 + 5 % H_2S + 5 % CH_4 (4C), and 85 % CO_2 + 5 % H_2S + 5 % CH_4 + 5 % N_2 (5C). The initial salinity, temperature, and pressure were kept consistent with the original SPE11C setup. The ASC algorithm demonstrates a small increase in RSAR as the gas composition becomes more complex. Despite this increase, the results highlight the significant computational efficiency of the ASC algorithm, with stability analysis reduced to less than 2.7 % of the original required stability analysis number. This substantial reduction in stability analysis is attributed to the relatively small proportion of grid cells swept by the CO_2 plume in the SPE11C model. The lower RSAR observed for the SPE11C model compared to the GMGHG005M cases suggests that the ASC algorithm is more effective in handling realistic geological storage models. Realistic models often include extensive regions where CO_2 does not reach, thereby requiring fewer necessary stability analyses. Notably, the ASC algorithm did not encounter any bad bypassing during the SPE11C simulations, further confirming its high accuracy and reliability. This eliminates concerns that stability analysis bypassing algorithms might compromise simulation accuracy, making the ASC algorithm a robust choice for geological carbon storage simulations. These findings reinforce the advantages of the ASC algorithm in handling both efficiency and accuracy, particularly in complex and real-world storage scenarios.

4. Conclusions

In this study, we proposed a novel stability analysis bypassing method for geological carbon storage simulations. Through extensive testing on a benchmark model (GMGHG005M) and a more realistic model (SPE11C), we evaluated the performance of the Adaptive Saturated Composition (ASC) algorithm. Our results show that stability analysis bypassing algorithms can substantially reduce the CPU time required for phase equilibrium calculations by minimizing the frequency of stability analyses, thus accelerating large-scale GCS simulations. The

ASC method achieved impressive bypassing efficiency, successfully skipping 93 %–99.9 % of unnecessary stability analyses across various scenarios, with the Residual Stability Analysis Ratio (RSAR) dropping below 0.1 % in simpler composition cases. Moreover, the ASC algorithm maintained excellent accuracy, as evidenced by a zero Binary Block Number (BBN) in all test cases, indicating no misclassification of two-phase conditions and eliminating concerns about accuracy loss due to bypassing. It also showed strong scalability, consistently delivering high performance across different gas compositions, which highlights its robustness in handling complex fluid systems in GCS applications. Compared to the shadow region bypassing (SB) method, the ASC algorithm exhibited superior performance by more effectively reducing RSAR and avoiding the misclassification issues commonly observed with SB, thereby offering a more reliable and efficient solution for phase equilibrium modeling in GCS simulations. Given its robust performance and broad applicability, the ASC algorithm holds great potential for integration into commercial reservoir simulators, enabling faster and more accurate modelling of large-scale GCS projects in practical engineering settings.

CRediT authorship contribution statement

Chaojie Di: Writing – original draft, Visualization, Software, Methodology, Formal analysis, Conceptualization. **Yizheng Wei:** Writing – review & editing, Software, Resources, Project administration. **Haoming Ma:** Writing – review & editing, Validation. **Peng Deng:** Validation, Data curation. **Benjieming Liu:** Resources. **Kun Wang:** Software. **Long Peng:** Validation, Data curation. **Zhangxin Chen:** Writing – review & editing, Supervision, Funding acquisition.

Data availability

The data supporting the findings of this study are available from the corresponding author upon reasonable request.

Declaration of competing interest

The authors declare that they have no known competing financial interests or personal relationships that could have appeared to influence the work reported in this paper.

List of Symbols, Abbreviations and Nomenclature

$a\alpha$	Dimensional attraction parameter
b	Dimensional repulsion parameters
c_i	Mole fraction of i-th component
c_s	Brine salinity
g	Gravity acceleration
$\boldsymbol{k}$	Absolute permeability
k_r	Relative permeability
k_{ij}	Binary interaction parameter (BIP)
N	Time step number
n	Component number
P_c	Critical pressure
q	Molar well flux
R	Universal gas constant
S	Phase saturation
T_r	Reduced temperature
$\boldsymbol{v}$	Phase volumetric velocity
v	Molar volume
Z	Grid depth
z_i	Feed mole fraction for i-th component
ρ	Molar density
ϕ	Rock porosity
η	Scaling factor in the SB method
Ω_a	Attraction parameter constant
ASC	Adaptive Saturated Composition
BBN	Bad Bypassing Number
BIP	Binary Interaction Parameters
CCUS	Carbon Capture, Utilization, and Storage
CPA	Cubic-Plus-Association
CPU	Central Processing Unit
CSAT	Compositional Space Adaptive Tabulation
CSF	Constant scaling factor
EOS	Equations of State
PR EOS	Peng-Robinson EOS
PR-SW EOS	PR EOS modified by Søride and Whitson
SRK EOS	Soave-Redlich-Kwong EOS
GCS	Geological Carbon Storage
MF	Mole Fraction
NB	Neighborhood Bypassing
OSF	Optimal Scaling Factor
PC-SAFT	Perturbed-Chain Statistical Associating Fluid Theory
PVT	Pressure-Volume-Temperature
RSAR	Residual Stability Analysis Ratio
SAN	Stability Analysis Number
SB	Shadow-region Bypassing
SMF	Saturated Mole Fractions
subscript	
g	Gas phase
w	Water phase
i	i-th component

Appendix A. Supplementary data

Supplementary data to this article can be found online at https://doi.org/10.1016/j.renene.2025.123545.

References

[1] S. Krevor, H. de Coninck, S.E. Gasda, N.S. Ghaleigh, V. de Gooyert, H. Hajibeygi, R. Juanes, J. Neufeld, J.J. Roberts, F. Swennenhuis, Subsurface carbon dioxide and hydrogen storage for a sustainable energy future, Nat. Rev. Earth Environ. 4 (2023) 102–118, https://doi.org/10.1038/s43017-022-00376-8.

[2] F. Chen, L. Yang, L. Tang, J. Gu, Comprehensive investigation of flue gas component separation and CO2 sequestration in water-saturated porous media of subsurface formation, J. Clean. Prod. 478 (2024), https://doi.org/10.1016/j.jclepro.2024.143951.

[3] J. Li, Y.M. Wei, M. Dai, Investment in CO2 capture and storage combined with enhanced oil recovery in China: a case study of China's first megaton-scale project, J. Clean. Prod. 373 (2022), https://doi.org/10.1016/j.jclepro.2022.133724.

[4] H. Ma, Y. Yang, Y. Zhang, Z. Li, K. Zhang, Z. Xue, J. Zhan, Z. Chen, Optimized schemes of enhanced shale gas recovery by CO2-N2 mixtures associated with CO2 sequestration, Energy Convers. Manag. 268 (2022) 116062, https://doi.org/10.1016/j.enconman.2022.116062.

[5] Z. Xue, H. Ma, Y. Wei, W. Wu, Z. Sun, M. Chai, C. Zhang, Z. Chen, Integrated technological and economic feasibility comparisons of enhanced geothermal systems associated with carbon storage, Appl. Energy 359 (2024), https://doi.org/10.1016/j.apenergy.2024.122757.

[6] E. Gabruś, K. Wojtacha-Rychter, T. Aleksandrzak, A. Smoliński, M. Król, The feasibility of CO2 emission reduction by adsorptive storage on Polish hard coals in the upper silesia coal basin: an experimental and modeling study of equilibrium, kinetics and thermodynamics, Sci. Total Environ. 796 (2021) 149064, https://doi.org/10.1016/j.scitotenv.2021.149064.

[7] S. Kumar, J. Foroozesh, K. Edlmann, M.G. Rezk, C.Y. Lim, A comprehensive review of value-added CO2 sequestration in subsurface saline aquifers, J. Nat. Gas Sci. Eng. 81 (2020), https://doi.org/10.1016/j.jngse.2020.103437.

[8] J.M. Nordbotten, M. Anthony Celia, Geological Storage of CO2 : Modeling Approaches for large-scale Simulation, Wiley, Hoboken, N.J, 2012.

[9] Z. Kou, Y. Xin, H. Wang, Y. Qu, Y. Li, H. Zhu, Exploring CO2 storage with impurities in deep saline aquifers through computational experiments, Renew. Energy 223 (2024) 120085, https://doi.org/10.1016/j.renene.2024.120085.

[10] I. Søreide, C.H. Whitson, Peng-robinson predictions for hydrocarbons, CO2, N2, and H2 S with pure water and NaCI brine, Fluid Phase Equilib. 77 (1992) 217–240, https://doi.org/10.1016/0378-3812(92)85105-H.

[11] C.M. Oldenburg, TOGA: a TOUGH Code for Modeling three-phase, multi-component, and Non-isothermal Processes Involved in CO2-based Enhanced Oil Recovery Lehua Pan, 2020.

[12] L.C. Young, Compositional reservoir simulation: a review, SPE J. 27 (2022) 2746–2792, https://doi.org/10.2118/208610-PA.

[13] Z. Chen, Guanren Huan, Yuanle Ma, Computational Methods for Multiphase Flows in Porous Media, Society for Industrial and Applied Mathematics, 2006.

[14] C. Di, Y. Wei, K. Wang, B. Liu, P. Deng, Z. Sun, X. Lei, Z. Chen, A parallel compositional reservoir simulator for large-scale CO2 geological storage modeling and assessment, Sci. Total Environ. 955 (2024), https://doi.org/10.1016/j.scitotenv.2024.177065.

[15] G. Hui, Z. Chen, R. Schultz, S. Chen, Z. Song, Z. Zhang, Y. Song, H. Wang, M. Wang, F. Gu, Intricate unconventional fracture networks provide fluid diffusion pathways to reactivate pre-existing faults in unconventional reservoirs, Energy (Calg.) 282 (2023), https://doi.org/10.1016/j.energy.2023.128803.

[16] M.L. Michelsen, The isothermal flash problem. Part II. Phase-split calculation, Fluid Phase Equilib. 9 (1982) 21–40, https://doi.org/10.1016/0378-3812(82)85002-4.

[17] M.L. Michelsen, The isothermal flash problem. Part I. Stability, Fluid Phase Equilib. 9 (1982) 1–19, https://doi.org/10.1016/0378-3812(82)85001-2.

[18] H. Cao, Development of Techniques for General Purpose Simulators, 2002.

[19] H. Pan, H.A. Tchelepi, Compositional flow simulation using reduced-variables and stability-analysis bypassing, in: SPE Reservoir Simulation Symposium, SPE, 2011, pp. 21–23, https://doi.org/10.2118/142189-MS.

[20] C.H. Whitson, M.R. Brulé, S. of Petroleum Engineers of Aime, Phase Behavior , Henry L. Doherty Memorial Fund of AIME, Society of Petroleum Engineers, Richardson, Tex, 2000.

[21] D.-Y. Peng, D.B. Robinson, A new two-constant equation of state, Ind. Eng. Chem. Fundam. 15 (1976) 59–64, https://doi.org/10.1021/i160057a011.

[22] G. Soave, Equilibrium constants from a modified redlich-kwong equation of state, Chem. Eng. Sci. 27 (1972) 1197–1203, https://doi.org/10.1016/0009-2509(72)80096-4.

[23] Z. Duan, R. Sun, An improved model calculating CO2 solubility in pure water and aqueous NaCl solutions from 273 to 533 K and from 0 to 2000 bar, Chem. Geol. 193 (2003) 257–271, https://doi.org/10.1016/S0009-2541(02)00263-2.

[24] S. Chabab, P. Théveneau, J. Corvisier, C. Coquelet, P. Paricaud, C. Houriez, E. El Ahmar, Thermodynamic study of the CO2–H2O–NaCl system: measurements of CO2 solubility and modeling of phase equilibria using soreide and whitson, electrolyte CPA and SIT models, Int. J. Greenh. Gas Control 91 (2019) 102825.

[25] A. Hassanpouryouzband, M.V. Farahani, J. Yang, B. Tohidi, E. Chuvilin, V. Istomin, B. Bukhanov, Solubility of flue gas or carbon dioxide-nitrogen gas mixtures in water and aqueous solutions of salts: experimental measurement and thermodynamic modeling, Ind. Eng. Chem. Res. 58 (2019) 3377–3394, https://doi.org/10.1021/acs.iecr.8b04352.

[26] CMG Ltd., CMG-GEM software. https://www.cmgl.ca/, 2024. (Accessed 1 August 2024).

[27] C. Di, Y. Wei, K. Wang, P. Deng, B. Chen, L. Shen, Z. Chen, The impact of pressurization-induced decrease of capillary pressure and residual saturation on geological carbon dioxide storage, J. Clean. Prod. 486 (2025), https://doi.org/10.1016/j.jclepro.2024.144573.

[28] P. Deng, Z. Chen, X. Peng, J. Wang, S. Zhu, H. Ma, Z. Wu, Optimized lower pressure limit for condensate underground gas storage using a dynamic pseudo-component model, Energy (Calg.) 285 (2023) 129505, https://doi.org/10.1016/j.energy.2023.129505.

[29] T. Ajayi, J.S. Gomes, A. Bera, A review of CO2 storage in geological formations emphasizing modeling, monitoring and capacity estimation approaches, Pet. Sci. 16 (2019) 1028–1063, https://doi.org/10.1007/s12182-019-0340-8.

[30] Z. Wang, J. Wang, C. Lan, I. He, V. Ko, D. Ryan, A. Wigston, A study on the impact of SO2 on CO2 injectivity for CO2 storage in a Canadian saline aquifer, Appl. Energy 184 (2016) 329–336, https://doi.org/10.1016/j.apenergy.2016.09.067.

[31] R. Gholami, A. Raza, S. Iglauer, Leakage risk assessment of a CO2 storage site: a review, Earth Sci. Rev. 223 (2021), https://doi.org/10.1016/j.earscirev.2021.103849.

[32] W. Xiong, L.-H. Zhang, Y.-L. Zhao, S.-M. Wen, K. Bao, O. Møyner, K.-A. Lie, Compositional Simulation for Carbon Storage in Porous Media Using an Electrolyte Association Equation of State, in: SPE Journal (Society of Petroleum Engineers (U. S.) : 1996), 2024, pp. 1–23.

[33] Schlumberger, ECLIPSE 300 Software, 2024.

[34] Schlumberger, ECLIPSE 100 Software, 2024.

[35] C. Di, K. Wang, Y. Wei, L. Shen, Z. Chen, A hybrid stability analysis bypassing method for compositional simulation, Comput. Geosci. (2023), https://doi.org/10.1007/s10596-023-10209-2.

[36] A. Belkadi, W. Yan, E. Moggia, M.L. Michelsen, E.H. Stenby, I. Aavatsmark, E. Vignati, Speeding up compositional reservoir simulation through an efficient implementation of phase equilibrium calculation, in: All Days, SPE, 2013, https://doi.org/10.2118/163598-MS.

[37] D. Voskov, H.A. Tchelepi, Compositional space parametrization for miscible displacement simulation, Transport Porous Media 75 (2008) 111–128, https://doi.org/10.1007/s11242-008-9212-1.

[38] D. Xie, T. Jiang, G. Ren, Z. Chi, D. Cao, T. He, Y. Liao, Y. Zhang, Feasibility analysis on the debrining for compressed air energy storage salt cavern with sediment, Renew. Energy 237 (2024) 121529, https://doi.org/10.1016/j.renene.2024.121529.

[39] J. Jiang, B. Zhang, W. Chen, X. Zhang, D. Li, J. Li, H. Li, X. Xue, Investigation and optimization of the thermal performance of compressed supercritical CO2 energy storage system based on dynamic modeling and transient simulation, Renew. Energy 238 (2025) 121966, https://doi.org/10.1016/j.renene.2024.121966.

[40] Y. Wu, P. Li, Y. Hao, A. Wanniarachchi, Y. Zhang, S. Peng, Experimental research on carbon storage in a CO2-Based enhanced geothermal system, Renew. Energy 175 (2021) 68–79, https://doi.org/10.1016/j.renene.2021.04.139.

[41] National Institute of Standards and Technology, NIST (national institute of standards and technology) chemistry WebBook. https://webbook.nist.gov/chemistry/, 2025. (Accessed 23 March 2025).

[42] J.M. Nordbotten, M.A. Ferno, B. Flemisch, A.R. Kovscek, K.-A. Lie, The 11th Society of Petroleum Engineers Comparative Solution Project: Problem Definition, in: 2024 SPE Journal, vol. 1, 2024, https://doi.org/10.2118/218015-PA/3341981/spe-218015-pa.pdf/1.